Quantum Theory of Fractional Topological Pumping of Lattice Solitons

Julius Bohm,[1] Hugo Gerlitz,[1] Christina Jörg,[1,2] and Michael Fleischhauer[1,2]
[1]*Department of Physics and Research Center OPTIMAS, RPTU University Kaiserslautern-Landau, 67663 Kaiserslautern, Germany*
[2]*Research Center QC-AI, RPTU University Kaiserslautern-Landau, 67663 Kaiserslautern, Germany*

(Received 5 September 2025; accepted 26 January 2026; published 26 February 2026)

One of the hallmarks of topological systems is the robust quantization of particle transport. It is the origin of the integer-valued quantum Hall conductivity and a potential tool for quantum information technology. Recent experiments on topological pumps constructed by using arrays of photonic waveguides and described by the (lattice-translational invariant) Aubry-André-Harper model, have demonstrated both integer and fractional transport of lattice solitons. In these systems, a background medium mediates interactions between photons via a Kerr nonlinearity and leads to the formation of self-bound multiphoton states. Upon increasing the interaction strength, a sequence of transitions was observed from a phase with integer transport in a pump cycle through different phases of fractional transport to a phase with no transport. We here present a quantum description of topological pumps of self-bound many-particle states in terms of an effective Hamiltonian of their center-of-mass (c.m.) motion, which allows one to introduce an effective band structure $E_\mu(K)$ with K being the c.m. momentum and to classify topological phases in terms of generalized symmetries. We provide an explicit analytic expression of the effective Hamiltonian for few particles in the strong interaction limit and present numerical results in the more general case. We identify a topological invariant, an effective single-particle Chern number, which fully governs the soliton transport. Increasing the interaction strength in the Aubry-André-Harper model leads to a successive merging of c.m. bands, which is the origin of the observed sequence of topological phase transitions and also the potential breakdown of topological quantization for some interaction strength.

DOI: 10.1103/hhgy-9rd4

Subject Areas: Condensed Matter Physics, Quantum Physics, Topological Insulators

I. INTRODUCTION

Topological quantum systems have been intensively studied since the discovery of the quantum Hall effect [1]. One of the simplest examples for such systems is a Thouless pump [2], which displays a quantized particle transport in an insulating bulk state of a 1D translationally invariant lattice upon cyclic adiabatic changes of system parameters. The transport is governed by an integer topological invariant, equivalent to a Chern number. The quantization of transport not only applies to a fully filled fermion band, it is also observable in the center-of-mass motion of a single particle equally distributed over all momentum states (see, e.g., Ref. [3] for a detailed overview.) A major problem in the single-particle case is the fast dispersion of the wave function. A possible solution for this has been utilized in Refs. [4–6] using bound many-particle objects: lattice solitons. They show quantized transport in a topological pump while being almost nondispersive due to their large mass. The notion solitons is used here colloquially, as the self-bound many-particle states may not fulfill all properties of true solitons [7–9]. In the experiments of Ref. [6], laser pulses have been injected into spatially modulated waveguide arrays simulating a time-dependent Aubry-André-Harper (AAH) Hamiltonian with a Kerr nonlinearity mediating interactions [10–12]. Increasing the light intensity, solitons form, for which integer transport in a full pump cycle was observed. Above a certain power threshold, all transport is halted. In subsequent work [13], an interaction controlled transition between phases with integer and *fractional* transport was demonstrated (see Fig. 1).

These observations triggered an extended body of theoretical work [14–20] based on the discrete nonlinear Schrödinger equation (DNLSE) [21]. While the DNLSE accurately reproduces the observed shift in the c.m. and relates the transition points between phases of different fractional transport to bifurcation points of soliton

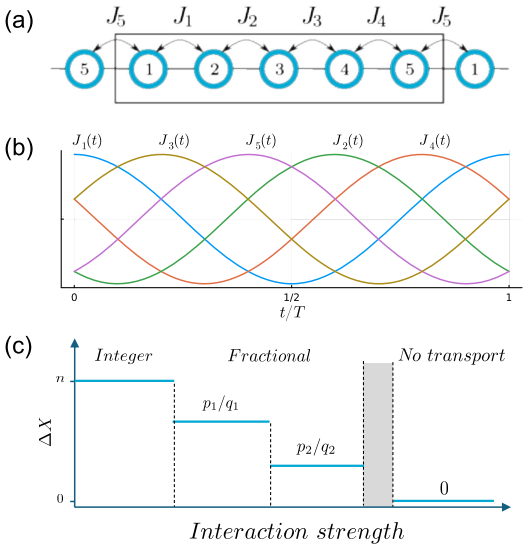

FIG. 1. (a),(b) 1D Aubry-André-Harper model with modulated hopping rates $J_1(t)\ldots J_5(t)$ and on-site interactions U. (c) Motion of center of mass of a soliton ΔX in a pump cycle. Upon increasing the interaction strength, there are multiple transitions between phases of integer, fractional, and eventually absent transport, in some cases intersected by a small interval of nonquantized transport (gray area).

solutions, the underlying mean-field description fails to provide an explanation for the quantized transport in terms of a topological invariant and of the origin of the topological phase transitions.

Using perturbation theory, it has been argued in Refs. [14,16] that for weak interactions the position of the soliton follows that of the Wannier centers of the single-particle band from which the soliton bifurcates and, thus, is governed by the Chern number of this band. However, as shown in Sec. II B, there is a gradually growing admixture of higher single-particle bands when the interaction is increased, and the perturbative arguments fail entirely in the fractional case. We note that there are approaches introducing nonlinear winding numbers [15,20] or Chern numbers [19] to characterize topological properties of the mean-field solutions also in the regime of large nonlinearities. These approaches are, however, limited to systems with certain symmetries or capture only special nonlinear solutions which do not include self-bound solutions such as solitons or time-dependent Hamiltonians. Finally, cases of anomalous nonlinear Thouless pumping were found [22], and in Ref. [23] it was predicted that multicomponent solitons can show fractional transport, despite the fact that the single-particle bands are all topologically trivial. This shows that the topological transport of solitons cannot be traced back to topological properties of the underlying single-particle Hamiltonian. Most recently, a fermionic model with repulsive interactions has been investigated [24], where fractional transport emerges from coupling of single-particle bands by repulsive interactions of fermions.

We here unravel the origin of the quantized soliton transport and provide an explanation for the observed phase transitions by developing a fully quantum description of topological soliton pumps. To be specific, we consider the AAH model as a generic example; the approach applies, however, to all systems with self-bound many-particle states in a translationally invariant lattice model. We show that the topological contribution to their transport can be described in terms of an effective single-particle Chern number, provided the soliton solution is gapped from all extended (not self-bound) many-body states. Introducing an effective single-particle Hamiltonian for solitons, which due to translational invariance can be characterized by an effective soliton band structure, we show that in the AAH model for increasing interaction strength different soliton bands merge at some parameter values of the pump cycle. At this point, the transport is governed by a Wilson loop, giving rise to different phases with fractionally quantized average transport. Increasing the interaction further eventually mixes all soliton bands, and, since the total Wilson loop of all soliton c.m. bands must vanish, the topological transport collapses [6,25]. For single-particle Bloch Hamiltonians also particles prepared in excited bands show quantized topological transport, determined by the corresponding Chern number. We show that an analogous behavior can be observed for solitons if the system is prepared in an excited soliton band that is stable and has a finite band gap to lower- (and higher-) lying solutions.

Finally, we show that in some intermediate interaction regimes the energetically highest of a set of crossing soliton bands may be degenerate with bands of extended states. In such a case, the transport is no longer (fractionally) quantized and may take arbitrary values, explaining the fluctuating transport numerically predicted in Ref. [17]. Since the effective Hamiltonian of solitons is a single-particle Hamiltonian, its symmetries under time reversal, charge conjugation, and chiral transformation provide a full classification of possible topological phases according to Refs. [26,27].

II. MODEL AND MEAN-FIELD APPROACH

A. Aubry-André-Harper model

We consider a generic lattice model with attractive on-site interactions. Specifically, we investigate the bosonic tight-binding Hamiltonian

$$\begin{aligned}\mathcal{H}(t) &= \mathcal{H}_0(t) + \mathcal{H}_{\mathrm{int}} \\ &= -\sum_l \Big[\left(J_l(t)\hat{a}_l^\dagger \hat{a}_{l+1} + \mathrm{H.c.}\right) \\ &\quad + \epsilon_l(t)\hat{a}_l^\dagger \hat{a}_l + \frac{U}{2}\hat{n}_l(\hat{n}_l - 1)\Big], \end{aligned} \tag{1}$$

where $\mathcal{H}_0$ describes the single-particle dynamics in the lattice and is periodic in time with period T,

i.e., $\mathcal{H}_0(t) = \mathcal{H}_0(t+T)$. The corresponding hopping amplitudes J_l and on-site energies ϵ_l have a spatial period p, which defines the unit-cell size. $\mathcal{H}_{\rm int}$ describes an (attractive) on-site interaction of strength $U > 0$, which will be parametrized as $U = U_0/N$ with N being the total number of particles. In order to understand the emergence of topological phase transitions observed in Refs. [6,13], we consider specifically the 1D Aubry-André-Harper model [10,11] with hopping amplitudes

$$J_l(t) = J\left(1 + \delta\cos\left(\Omega t + \frac{2\pi l k}{p}\right)\right), \tag{2}$$

with $0 < \delta < 1$; see Fig. 1.

The spatial period p is chosen to be a prime number so that it is never commensurable with l and/or k, which would effectively reduce the spatial period. The phase offset k, which is chosen to be smaller than $p/2$, determines the smallest possible fraction in the topological transport. If not explicitly stated otherwise, we choose a spatial period $p = 5$ and a phase offset $k = 2$. This is the smallest possible unit-cell size where fractional transport appears in the AAH chain. All on-site potentials ϵ_l in Eq. (1) are chosen to be 0.

With periodic boundary conditions, the Hamiltonian is translational invariant, i.e., $\hat{T}\mathcal{H}\hat{T}^{-1} = \mathcal{H}$, where $\hat{T}$ is the translation operator by one unit cell, i.e., $\hat{T}\hat{a}_l\hat{T}^{-1} = \hat{a}_{l+p}$. As a consequence, the lattice momentum K of the center of mass (c.m.) is a conserved quantity.

Attractive interactions U lead to localized soliton states. These are states with a distribution of occupation numbers that decay with increasing distance to the center of mass with a localization length ξ, i.e., $\langle\hat{n}_{l+d}\hat{n}_l\rangle \sim \exp\{-|d|/\xi\}$ for $d \gg 1$. We call them *stable* if they have an energy gap to all extended states with the same K. On the quantum level, a minimum value U_c is required for a soliton to form, which tends to zero as $N \to \infty$ [28]. In a complex energy structure, multiple soliton solutions can exist, which for some parameter values may become degenerate. Furthermore, stable excited soliton solutions may not exist at all times, as they can become degenerate with extended states in some parts of the pump cycle. In this case, we call these solitons partially stable.

B. Mean-field approach: Discrete nonlinear Schrödinger equation

In mean-field approximation, the dynamics of solitons in a 1D lattice are described by the discrete nonlinear Schrödinger equation. This equation can be obtained from a Gutzwiller coherent-state ansatz [29] for the many-body quantum state

$$|\psi\rangle = \prod_l |\phi_l\rangle, \quad \text{where } \hat{a}_l|\phi_l\rangle = \phi_l|\phi_l\rangle.$$

For the AAH Hamiltonian [Eq. (1)], it reads ($\hbar = 1$)

$$i\frac{\partial}{\partial t}\phi_l = -J_l\phi_{l+1} - J_{l-1}\phi_{l-1} - \epsilon_l\phi_l - U|\phi_l|^2\phi_l. \tag{3}$$

Numerical simulations of Eq. (3) have provided a good description of soliton energies and the observed soliton transport in parameter regimes where the soliton is stable. The semiclassical description, however, fails to explain the topological nature of the transport and the origin of topological phase transitions. In Refs. [14,16], it was argued that for weak interactions the solitons can be represented in terms of the most localized Wannier states of single-particle Bloch bands neglecting exchange terms between the latter. Under this assumption, the topological transport is described by the Chern number of the Bloch band the soliton bifurcates from.

In Fig. 2, we have plotted the integrated overlap of a soliton obtained from a self-consistent solution of Eq. (3) with the single-particle Bloch wave functions for the two lowest bands for the AAH model with phase offset $k = 2$ and unit-cell size $p = 5$ as a function of interaction strength U/J. The vertical spread of data points reflects different times in the pump cycle. One recognizes that, while in the perturbative limit of very small absolute values of interaction strengths there is indeed a close to unity overlap with the lowest Bloch band, contributions from higher bands continuously grow with increasing interaction strength. In particular, both in experiments and in numerical simulations of the DNLSE, integer transport is seen up to rather large interaction strength at which the admixture of higher Bloch bands is already quite substantial. Moreover, in the regime of fractional transport, following the above argument, one would expect equal contributions from the lowest and the first excited band, which is clearly not the case. Therefore, the resulting topological invariant is not just the average of the single-particle Chern numbers.

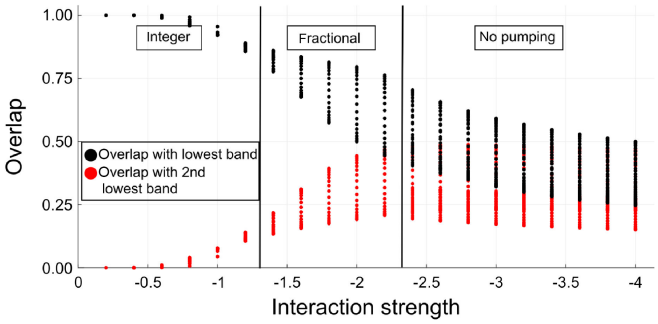

FIG. 2. Overlap of eigensolution of the DNLSE [Eq. (3)] for the AAH model with phase offset $k = 2$ and unit-cell size $p = 5$ with single-particle Bloch bands for different interaction strength U/J. Data points for the same interaction strength correspond to different times in the pumping cycle.

III. CENTER-OF-MASS TRANSPORT AND MANY-BODY CHERN NUMBER

Since the semiclassical approaches to describe the transport of lattice solitons were shown to be incomplete, we here derive a quantum mechanical description. Specifically, we are interested in the transport of the c.m. of a soliton when $\mathcal{H}_0(t)$ is adiabatically varied over a period T, where the translational invariance is not changed. The instantaneous eigenstates of $\mathcal{H}(t)$ can be classified in terms of the conserved c.m. momentum K and a band index μ and are denoted as $|E_\mu(K)\rangle$ with energy $E_\mu(K)$.

The time evolution of the center-of-mass position of the N particles, $\hat{X} = \sum_{j=1}^{N} \hat{x}_j/N$, is governed by the N-particle velocity operator $\partial_t \hat{X} = \hat{V} = -i[\hat{X}, \mathcal{H}] = -i[\hat{X}, \mathcal{H}_0]$, which can be conveniently expressed in terms of a momentum-shifted Hamiltonian $\mathcal{H}(q) = e^{-iq\hat{X}}\mathcal{H}e^{iq\hat{X}}$. In other words, $\hat{V} = \hat{V}(q)|_{q=0}$ with $\hat{V}(q) = e^{-iq\hat{X}}\hat{V}e^{iq\hat{X}} = \partial\mathcal{H}(q)/\partial q$.

$$\frac{d}{dt}\langle\hat{X}\rangle = \langle\hat{V}(q)\rangle_{q=0} = \left\langle\frac{\partial\mathcal{H}(q)}{\partial q}\right\rangle_{q=0}. \tag{4}$$

In the following, we discuss the topological contributions to $d\langle\hat{X}\rangle/dt$ for degenerate and nondegenerate solutions separately.

A. Nondegenerate soliton solutions

Let us first consider a nondegenerate soliton solution; i.e., for a given c.m. momentum K, there is only one eigenstate for each energy value in the whole pump cycle. In order to calculate the transport of a soliton from a single nondegenerate band, one can follow the well-known arguments for the transport of a single particle [2,30]. To account for the topological transport starting in an instantaneous eigenstate $|E_0(K,t)\rangle$ at time t, one has to take into account nonadiabatic corrections. As the modulation of the Hamiltonian does not affect the translational invariance, nonadiabatic transitions couple only to states with the same c.m. momentum. Nondegenerate time-dependent perturbation theory yields

$$|\Psi(K,t)\rangle = |E_0(K)\rangle + i\sum_{\alpha\neq 0}|E_\alpha(K)\rangle\frac{\langle E_\alpha(K)|\partial_t E_0(K)\rangle}{E_\alpha(K)-E_0(K)}, \tag{5}$$

where we have suppressed the dependence on time for notational simplicity. We note that $|\partial_t E_0(K)\rangle$ is orthogonal to $|E_0(K)\rangle$ and that the second term in the above expression is small. Calculating the average velocity in this state gives in lowest order of perturbation theory

$$\begin{aligned}\langle\hat{V}(q=0,t)\rangle &= \frac{\partial E_0(K)}{\partial K} + i\sum_{\alpha\neq 0}\left(\frac{\langle E_0|\partial_q\mathcal{H}(q)|_{q=0}|E_\alpha\rangle\langle E_\alpha|\partial_t E_0\rangle}{E_\alpha - E_0} - \text{c.c.}\right)\\ &= \frac{\partial E_0(K)}{\partial K} + i\left(\left\langle\frac{\partial E_0}{\partial t}\middle|\frac{\partial E_0}{\partial K}\right\rangle - \text{c.c.}\right).\end{aligned} \tag{6}$$

For the second step, we used

$$\begin{aligned}0 &= \partial_q\langle E_0|\mathcal{H}(q)|E_\alpha\rangle\\ &= \langle E_0|\partial_q\mathcal{H}(q)|E_\alpha\rangle + E_0\langle E_0|\partial_q E_\alpha\rangle + E_\alpha\langle\partial_q E_0|E_\alpha\rangle\end{aligned} \tag{7}$$

as well as

$$0 = \partial_q\langle E_0|E_\alpha\rangle = \langle E_0|\partial_q E_\alpha\rangle + \langle\partial_q E_0|E_\alpha\rangle. \tag{8}$$

The first term in Eq. (6) is just the group velocity of the band and describes the dynamical contribution to the transport. If we consider an initial soliton state with coefficient $c(K)$ in momentum state $|E_0(K)\rangle$, which is symmetric with respect to $K = 0$, the dynamical contribution vanishes. Then, the shift of the center of mass of the soliton in one period T is given by the second term in Eq. (6) integrated over all c.m. momenta K:

$$\Delta\langle\hat{X}\rangle = \int_0^T dt\int_{-\pi}^{\pi} dK|c(K)|^2\mathcal{F}(K,t). \tag{9}$$

Equation (9) is a weighted integral over the Berry curvature

$$\mathcal{F}(K,t) = i\left(\left\langle\frac{\partial E_0}{\partial t}\middle|\frac{\partial E_0}{\partial K}\right\rangle - \text{c.c.}\right) \tag{10}$$

in (K,t) space. In the special case, where the c.m. wave function of the soliton is initially localized to a single unit cell, all coefficients are equal, $|c(K)|^2 = 1/2\pi$. In this case, the transport is given by the effective single-particle Chern number of the soliton Bloch band; i.e., it is integer quantized:

$$\Delta\langle\hat{X}\rangle = \int_0^T dt\int_{-\pi}^{\pi}\frac{dK}{2\pi}\mathcal{F}(K,t) = C. \tag{11}$$

Note that we did not make any assumption about the many-body wave function other than its gapfulness. In particular, no assumption about its behavior in the *relative* coordinates of the particles was made. However, the assumption of gapfulness of the N-particle state with fixed c.m. momentum K requires, in general, that the N particles are bound to each other.

Finally, we comment on the relation between our description of soliton transport and other topological invariants for interacting many-body systems, such as the Niu-Thouless invariant [31]. The Niu-Thouless invariant employs twisted boundaries and is an integral over a

Berry curvature in (θ, t) space, with $\theta \in \{0, 2\pi\}$ being the twist angle. In contrast to $\mathcal{F}(K,t)$ [see Eq. (9)], a Berry curvature in (θ, t) would not describe the transport of an individual soliton but applies only to an insulating many-body state, such as a band insulator of noninteracting fermions, where all momentum states are equally occupied.

B. Degenerate soliton solutions

In the degenerate case, i.e., if there are crossings of m solutions at some points in time, we need to apply degenerate time-dependent perturbation theory to an m component vector $|\underline{\Psi}(K)\rangle = (|\Psi_0(K)\rangle, \ldots, |\Psi_{m-1}(K)\rangle)^\top$ and can express the time-evolved state as [32]

$$|\underline{\Psi}(K,t)\rangle = \mathcal{T} \exp\left\{-i \int_0^t d\tau \mathbf{A}_K(\tau)\right\} |\underline{\Psi}(K,0)\rangle + \text{nonadiabatic terms}, \tag{12}$$

where

$$\mathbf{A}_K(\tau) = \begin{pmatrix} E_0 & i\langle E_0|\partial_t E_1\rangle & i\langle E_0|\partial_t E_2\rangle & \cdots \\ i\langle E_1|\partial_t E_0\rangle & E_1 & i\langle E_1|\partial_t E_2\rangle & \cdots \\ i\langle E_2|\partial_t E_0\rangle & i\langle E_2|\partial_t E_1\rangle & E_2 & \cdots \\ \cdots & \cdots & \cdots & \cdots \end{pmatrix} \tag{13}$$

is the Wilczek-Zee non-Abelian Berry connection and "nonadiabatic terms" denotes the perturbative contributions due to nonadiabatic couplings to other, energetically separated states similar to the nondegenerate case. We note that since $\langle E_l|\partial_t E_m\rangle = (\langle E_l|\partial_t \mathcal{H}|E_m\rangle)/(E_m - E_l)$ [compare Eqs. (7) and (8)], the eigenstates of the matrix $\mathbf{A}_K$ coincide with the bare states $|E_0\rangle \ldots |E_m\rangle$ far away from the crossing point in the adiabatic limit. At the crossing point, the off-diagonal elements, however, diverge, in general, which leads to a mixing.

Suppose the cyclic change of the Hamiltonian starts at a point where there is no degeneracy between c.m. bands and the system is prepared in one solution, say, $|E_0(K)\rangle$. Then, in the presence of isolated crossing points with other solutions $|E_\alpha(K)\rangle$, a single cycle $t = 0 \to t = T$ will, in general, not return the initial state to itself, but multiple cycles are needed. Therefore, the topological transport is integer quantized only after multiple cycles, giving rise to a fractional average transport per cycle. In this case, where there are crossings of soliton solutions at some point in time, say, of $|E_0(K,t)\rangle$ and $|E_1(K,t)\rangle$, the Chern number must be generalized to a Wilson loop:

$$C_n = \frac{1}{2\pi} \int_0^T dt \partial_t \,\mathrm{Im}\,\log\,\det \mathbf{W}(t), \tag{14}$$

where $\mathbf{W}(t) = \mathcal{T} \exp\{i \int_{\mathrm{BZ}} dK \mathbf{B}_t(K)\}$ and

$$\mathbf{B}_t = \begin{pmatrix} \langle E_0|\partial_K E_0\rangle & i\langle E_0|\partial_K E_1\rangle \\ i\langle E_1|\partial_K E_0\rangle & \langle E_1|\partial_K E_1\rangle \end{pmatrix} \tag{15}$$

is the Wilczek-Zee non-Abelian Berry connection [32] for fixed time, here for $n = 2$ crossing bands. C_n is an integer, and the *average* topological transport per cycle in the n bands is given by C_n/n.

The c.m. transport of a soliton is then *fractional*, provided it returns to its original energy only after n periods. We show that this is the case for the Aubry-André-Harper model of Ref. [13].

IV. CALCULATING CHERN NUMBER AND WILSON LOOP OF SOLITONS

While the soliton energy structure can be well approximated by a self-consistent solution of the DNLSE, the many-body eigenstates and the Chern number [Eq. (11)] or the Wilson loop [Eq. (14)] must be obtained from solving the many-body Schrödinger equation, which constitutes a substantial challenge for more than a few particles. To tackle this problem, we introduce the following basis of states with a fixed K [33,34]:

$$|\Psi_\alpha(K)\rangle = \sum_{m=0}^{L-1} (e^{iK}\hat{T})^m |\Phi_\alpha(0;K)\rangle. \tag{16}$$

Here, we assume a lattice with L unit cells, each containing p sites, and periodic boundary conditions. The states

$$|\Phi_\alpha(0;K)\rangle = {\sum_{\{n_l\}}}' c_\alpha[\{n_l\};K]|\{n_l\}\rangle$$

describe the distribution of particles $n_l = \{n_{-pL/2+1} \ldots n_{pL/2}\}$ around the lattice site $l = 0$ (conveniently chosen close to the center of mass of all particles), with coefficients $c_\alpha[\{n_l\},K] = c_\alpha[n_{-pL/2+1} \ldots n_{pL/2};K]$ and $|\{n_l\}\rangle$ being a number state. We assume for simplicity that L is even. $\sum'_{\{n_l\}}$ denotes summation over all n_l's for which $\sum_l n_l = N$. Translation by a unit cell gives $\hat{T}|\Phi_\alpha(0,K)\rangle = |\Phi_\alpha(p,K)\rangle$. (Note that, in order to guarantee orthonormality, states $|n_{-\frac{pL}{2}+1}, \ldots, n_{\frac{pL}{2}}\rangle$ must not be eigenstates of $\hat{T}$.) Now we can make use of the fact that for large attractive interactions the solitons have a small localization length ξ. Thus, we can restrict ourselves to special cases: (i) two-site solitons where the basis states have at most two (neighboring) sites populated (i.e., $n_0, n_1 = N - n_0 \neq N$, in general) and (ii) three-site solitons where three adjacent lattice sites might be populated [i.e., $n_0, n_1, n_2 = N - (n_0 + n_1) \neq N$, in general]. In the basis of c.m. momenta K, the many-body Hamiltonian [Eq. (1)] is block diagonal; i.e., the c.m. momenta are decoupled. For the two-site solitons, the block dimension is $p \cdot N$; for the three-site soliton, it is $p \cdot N(N+1)/2$, which allows us to perform numerical

simulations for tens to hundreds of particles. Because of the limitation to two-site or three-site solitons, some of the higher-energy solutions are not true eigensolutions but are enforced by the boundary conditions. These states can be detected, however, by comparing two- and three-site solutions and are not relevant in the low-energy regime, discussed here.

In Fig. 3, we have plotted the energies of the solitons for the AAH model [Eq. (1)] and the c.m. transport as a function of time, for $N = 10$ particles with unit-cell size $p = 5$ and $U = 0.1$ for phase offsets $k = 1$ and $k = 2$. (Note that the soliton bands are almost flat with a bandwidth less than the width of the lines.) In the first case [Figs. 3(a) and 3(b)], there is a single lowest-energy soliton solution with many-body Chern number [Eq. (11)] $C = 1$ and integer transport. In the second case [Figs. 3(c) and 3(d)], two energies cross with a nontrivial Wilson loop [Eq. (14)] $C_2 = 1$ giving rise to fractional transport of $1/2$. The data are calculated within the three-site soliton ansatz.

With the same approach, we can numerically calculate the Berry curvature $\mathcal{F}(K,t)$ and from this the Chern number or Wilson loop. In Fig. 4, we have given an example for the Berry curvature of the AAH model with $N = 3$ particles, a $p = 5$ unit cell, and a $k = 1$ phase offset, which shows integer quantized transport similar to Fig. 3. Using Eq. (11) for this Berry curvature yields a c.m. Chern number $C = 1$. The yellow lines in Fig. 4 are numerical relicts and do not influence the result of the integration, since they are effectively sets of measure zero.

We here showed the applicability of our c.m. approach to identify the different topological phases. In the following, we provide an explanation for the phase transitions.

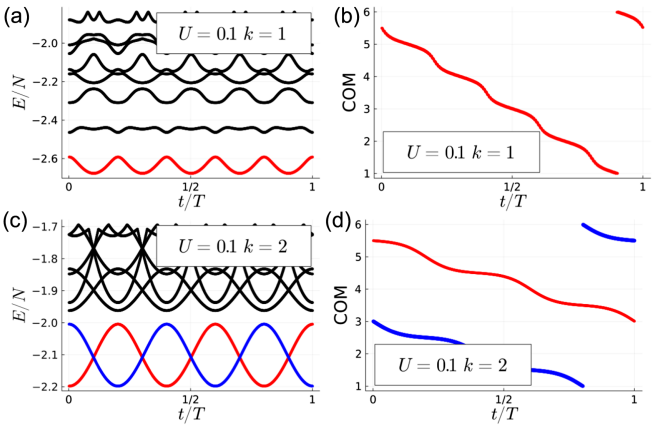

FIG. 3. Instantaneous soliton energies for ten particles for attractive interaction $U/J = 0.1$ with phase offset $k = 1$ in (a) and with phase offset $k = 2$ in (c) and unit-cell size $p = 5$. Note that the soliton bands are almost flat and the variation of $E(K)$ with K is less than the width of the lines. The corresponding c.m. movements in a pump cycle of the red and blue marked energies are shown in (b) and (d). The energies and c.m. positions are obtained with the three-site soliton ansatz.

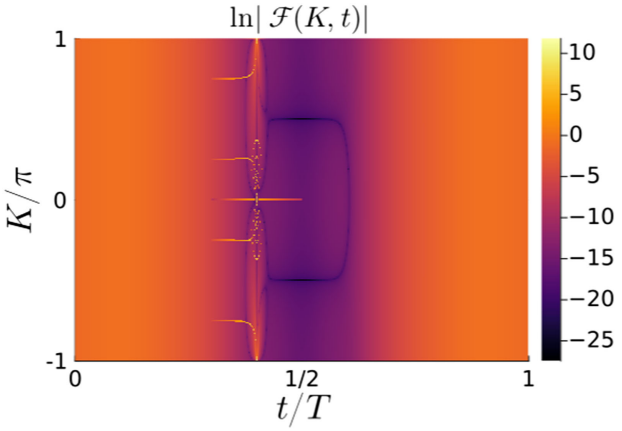

FIG. 4. Logarithm of the absolute value of the Berry curvature $\ln|\mathcal{F}(K,t)|$ in the lowest-energy solution for $N = 3$ particles, a $p = 5$ unit cell, and a $k = 1$ phase offset. Integrating Eq. (11) with this Berry curvature yields a Chern number $C = 1$. The sharp peaks, where $\ln|\mathcal{F}(K,t)|$ is on the order of 10, are numerical relicts but are effectively a set of measure zero for the integration.

V. TOPOLOGICAL PHASE TRANSITIONS

A. Effective soliton Hamiltonian

The c.m. dynamics of bound N-particle objects (solitons) can be described by an effective single-particle Hamiltonian with eigenstates $|E_\mu(K)\rangle$:

$$\mathcal{H}_{\text{eff}} = \sum_\mu \sum_K E_\mu(K)|E_\mu(K)\rangle\langle E_\mu(K)|. \tag{17}$$

Since such a model misses out the continuum of extended states, it is adequate only for stable soliton solutions. Defining annihilation and creation operators for solitons centered at lattice site l as $\hat{d}_l$ and $\hat{d}_l^\dagger$, respectively, the effective soliton Hamiltonian would read in coordinate space

$$\mathcal{H}_{\text{eff}}(t) = -\sum_l \left[(J_{l,\text{eff}}(t)\hat{d}_l^\dagger \hat{d}_{l+1} + \text{H.c.}) + \epsilon_{l,\text{eff}}(t)\hat{d}_l^\dagger \hat{d}_l \right], \tag{18}$$

where the $J_{l,\text{eff}}$ are the effective hopping rates of the soliton and the $\epsilon_{l,\text{eff}}$ effective local energies. (Note that we here have assumed only nearest-neighbor hopping.) All topological properties, including the topological classification according to the Altland-Zirnbauer scheme [26,27], as well as all phase transitions of solitons are determined by this effective Hamilton.

In the limit of strong attractive interactions, all soliton solutions have a localization length of a single lattice constant; i.e., all particles are located at the same lattice site. In this limit, we can explicitly derive the effective

Hamiltonian from perturbation theory. Furthermore, it is obvious that in this limit the number of soliton bands is the same as the number of single-particle bands. We explicitly construct $\mathcal{H}_{\text{eff}}$ for $N = 3$ particles in the strong interaction limit in Sec. VI. Here, we first discuss some of its general properties.

In the Aubry-Andre-Harper model [Eq. (1)], any small attraction U_0 is sufficient to form a bound state (lattice soliton) with an energy below the continuum of extended N-particle states, if N is large. Increasing the attractive interaction, the energy of these solitons is lowered and the bands deform. Moreover, excited soliton solutions can emerge. If the soliton bands have a nontrivial Chern number or Wilson loop, (fractional) quantized topological transport can be observed [6,13].

B. Merging of soliton bands

The experiments in Refs. [6,13] and DNLSE simulations showed that, for very large but still finite values of the interaction, the topological transport stops altogether. This can be understood as follows: For $U \gg J$, the localization of all soliton solutions is reduced to a single lattice site. Thus, the contribution of the local interaction to the energy, $UN(N-1)/2$, is the same for all solitons. Using a perturbative ansatz, one can show that, moreover, the contribution of the kinetic energy can be disregarded, as it scales as $\sim J(J/U)^{N-1}$ (see the Appendix and Ref. [35]). Thus, the effective soliton Hamiltonian becomes approximately diagonal and is entirely determined by local energies $\epsilon_{l,\text{eff}}$, which for the AAH model result from virtual hopping processes of a single particle from the soliton site l to an empty neighboring site (and back) and are in second-order perturbation theory proportional to $\epsilon_l \sim [J_l^2(t) + J_{l+1}^2(t)]/U$. As a consequence, all soliton bands cross at different points of the pump cycle and the topological transport is given by the total Wilson loop of all c.m. bands, which is always zero for general reasons.

The two limiting cases show that, as U is increased, initially separated soliton solutions must approach each other and eventually merge. As shown in Fig. 5, obtained from exact diagonalization simulations of a small system (30 lattices sites), they do so by forming Dirac-like cones which touch at a critical interaction U_c. In this case, the Chern numbers of the lowest two soliton bands are no longer adequate topological invariants, but one has to consider the Wilson loop. The topological transport can then become fractional, provided the soliton solutions which started at $t = 0$ are energetically well separated and switch bands at the Dirac-like points. We now show that this is indeed the case.

When the two soliton bands touch, the adiabatic evolution is governed by a U(2) transformation [32] [compare

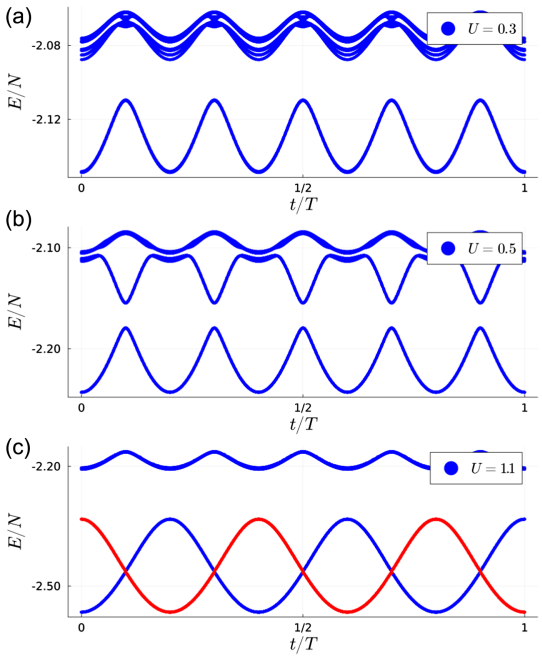

FIG. 5. Merging of soliton energies obtained from exact diagonalization with increasing interaction strength U for $N = 3$ particles, a $p = 5$ unit cell, and $k = 2$ phase offset. The number of unit cells is $L = 6$. A soliton originally prepared at $t = 0$ in one of the two bands will remain in this band if the changes are adiabatic and the soliton energies do not touch [(a) and (b)]. Once the energies touch in Dirac-like cones, the solutions switch bands at every crossing [red curve in (c)]. The width of the lines is larger than the width of the soliton bands in K space.

Eq. (12) in Sec. III B]

$$|\underline{\Psi}(K,t)\rangle = \mathcal{T}\exp\left\{-i\int_0^t d\tau \mathbf{A}_K(K,\tau)\right\}|\underline{\Psi}(K,0)\rangle. \quad (19)$$

Close to the crossing points, which we assume to take place at $t = t_0$, the non-Abelian Berry connection $\mathbf{A}_K$ takes on the form

$$\mathbf{A}_K = \begin{pmatrix} a|\tau| & -\frac{ib}{\tau} \\ \frac{ib}{\tau} & -a|\tau| \end{pmatrix}, \quad (20)$$

with $\tau = t - t_0$. Here, we assumed that apart from a common energy offset $E_0 = -E_1 = a|\tau|$, and, thus, $\langle E_0|\partial_t\mathcal{H}|E_1\rangle/(E_1 - E_0) \approx b/\tau$. Because of the diverging off-diagonal elements, the eigensolutions no longer follow the original solutions but cross from one to the other [see color code in Fig. 5(c)]. Since p is a prime number, there is an odd number of crossing points in one period in the AAH model. Thus, two periods are required for a soliton to return to the solution it started from. The shift in the c.m. position is then integer quantized only after two periods and the average transport per cycle is fractionally quantized. This

integer-to-fractional transition is sharp; i.e., it does happen without a region of nonquantized transport in between the two phases. The following section, however, discusses a situation where an intermediate region of nonquantized transport appears.

C. Failure of transport quantization

Based on solutions of the mean-field DNLSE, it was shown in Ref. [17] for the example of the Rice-Mele model [36–38] with local attractive interactions that the transition between quantized topological pumping of a soliton to zero pumping upon increasing the interaction strength may go through an intermediate regime of nonquantized transport. This transient failure of transport quantization, where $\langle \Delta \hat{X} \rangle$ strongly fluctuates, was attributed in Ref. [17] to a "self-crossing" of solutions of the semiclassical DNLSE. This phenomenon can be easily understood in the full quantum picture. For intermediate interactions, the excited soliton solution is in some parts of the pump cycle degenerate with the continuum of extended states and, thus, unstable. If this solution merges with the lower soliton band, the time evolution is no longer adiabatic and the transport is not quantized until the interaction is large enough such that also the excited band becomes fully gapped. In Fig. 6, we show the soliton energies in the Rice-Mele model with different values of the attractive on-site interaction U obtained from exact diagonalization simulations of a $N = 4$ soliton. The width of the lines reflects the width of the soliton bands $E(K, t)$ in K space. Although only marginally visible due to finite-size effects, Fig. 6(b) indicates the existence of a parameter range where the lowest soliton band becomes degenerate with an unstable excited solution leading to a fluctuating, nonquantized transport.

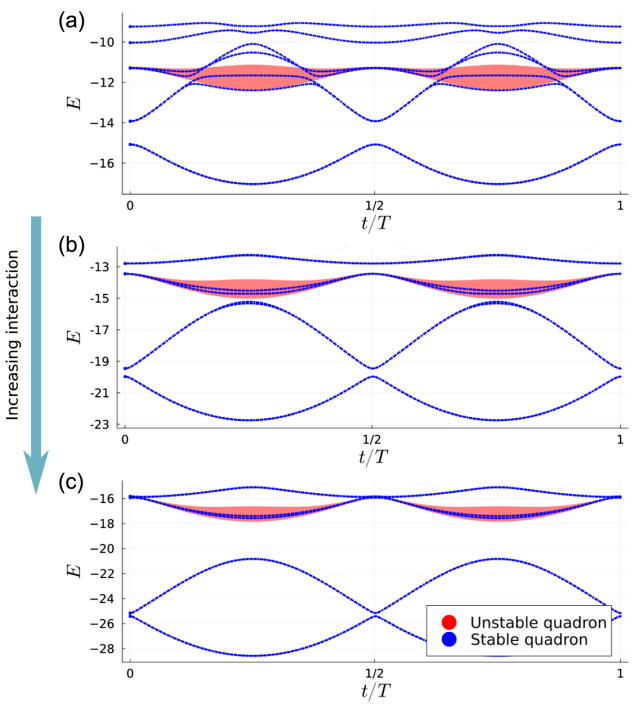

FIG. 6. Breakdown of transport quantization in the Rice-Mele model for intermediate values of on-site interactions. Shown are lowest energies for $N = 4$ bosons. (a) $U = 2.0$: the lowest soliton (quadron) band is gapped with Chern number $C = 1$ ($\langle \Delta \hat{X} \rangle = 1$). (b) $U = 3.0$: the lowest two bands merge but (except for finite-size effects) overlap with extended states (unstable quadron) where the transport is not quantized. (c) $U = 4.0$: the lowest two quadron bands merge with vanishing Wilson loop ($\langle \Delta \hat{X} \rangle = 0$). The width of the lines reflects the width of the soliton bands in K space.

VI. EFFECTIVE HAMILTONIAN: TRIPLON MODEL

As stated in Sec. V A, we can explicitly construct the effective soliton Hamiltonian in the strongly interacting limit where the noninteracting part of the Hamiltonian [Eq. (1)] can be treated as a small perturbation and the solitons become maximally localized (i.e., with a localization length ξ smaller than the lattice spacing).

In this limit, the binding energy $(U/2)N(N-1)$ is equal for all soliton solutions and is disregarded. Transport of the composite object occurs through collective hopping of particles, arising in Nth-order perturbation theory, which has a very small effective amplitude of $\sim J^N/U^{N-1}$ [35]. At the same time, virtual hopping processes of particles from the soliton site to a neighboring site and back give rise to local energy shifts with an amplitude proportional to $\sim J^2/U$. As shown in detail in the Appendix, this results in the effective energies and hopping amplitudes

$$\epsilon_{l,\mathrm{eff}} = \frac{3}{2}\frac{J_{l-1}^2 + J_l^2}{U}, \qquad J_{l,\mathrm{eff}} = \frac{3}{2}\frac{J_l^3}{U^2} \tag{21}$$

for the triplon model (i.e., $N = 3$). (For effective Bloch Hamiltonians of bound doublons and their topological features, see also Refs. [39–41]).

$$\mathcal{H}_{\mathrm{eff}}(t) = -\sum_l [[J_{l,\mathrm{eff}}(t)\hat{d}_l^\dagger \hat{d}_{l+1} + \mathrm{H.c.}] + \epsilon_{l,\mathrm{eff}}(t)\hat{d}_l^\dagger \hat{d}_l]. \tag{22}$$

In Fig. 7, we have shown the soliton energies of the effective triplon model for two different interaction strengths for the AAH model along with the integrand of the Wilson loop in Eq. (14) $\mathcal{W}_m = \mathrm{Im}\ \log\ \det \mathbf{P}(t)$, where m is the number of crossing bands. One clearly sees that for increased interaction strength the bands merge. Eventually, all five bands cross and there is no winding of $\mathcal{W}_5$; i.e., the total Wilson loop vanishes. Thus, despite the fact that the soliton mass is still finite, the topological transport vanishes exactly.

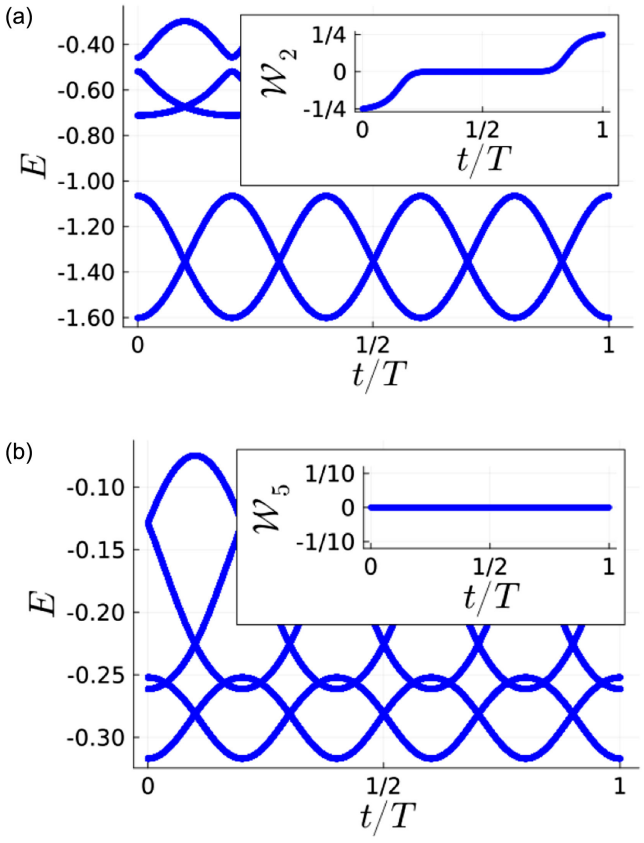

FIG. 7. Instantaneous soliton energies of the effective triplon model [Eq. (21)] for attractive interaction $U = 5$ in (a) and $U = 20$ in (b), phase offset $k = 2$, and unit-cell size $p = 5$. The inset shows the winding of $\mathcal{W} = \mathrm{Im}\ \log\ \det \mathbf{P}(t)$ [Eq. (14)], determining the Wilson loop.

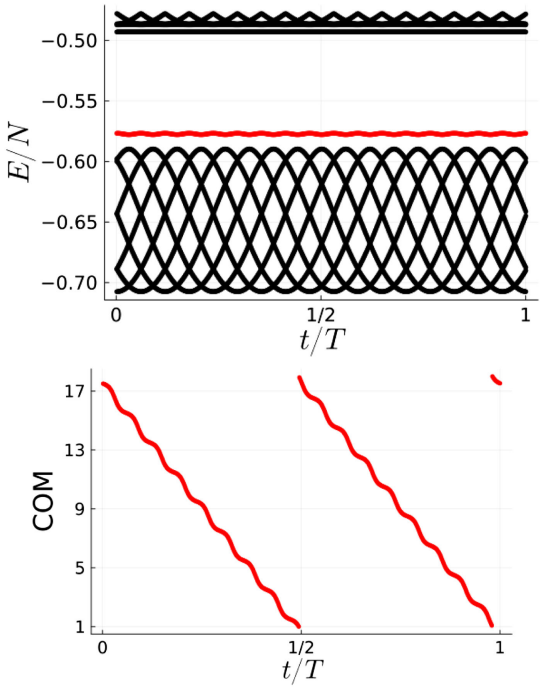

FIG. 8. Instantaneous soliton energies for three particles for attractive interaction $U/J = 1/3$ with phase offset $k = 8$ and unit-cell size $p = 17$ with the corresponding c.m. movement in a pump cycle of the red marked energy. The solutions are obtained with the three-site soliton ansatz.

The doublon model ($N = 2$) can also be treated analytically and, depending on the lattice model, can as well show an integer, fractional, or trapped case. But, since in the doublon case both the effective hopping and the effective potential are of the same order in interaction strength U^{-1}, there is no qualitative change of the band structure and, therefore, no phase transition.

Furthermore, while the dispersion of wave packets during a topological pump can be suppressed also for single particles in lattices with weakly dispersive (or flat) bands [42], the interaction-driven topological phase transitions, discussed here, require virtual hopping processes which do not exists in single-particle systems. Thus, these transitions are a remarkable and unique feature of composite particles (with more than two particles).

VII. TOPOLOGICAL TRANSPORT IN HIGHER SOLITON BANDS

So far, we mainly discussed the behavior of ground-state solitons. In single-particle Thouless pumps (like the AAH model without interaction), quantized topological transport also occurs in higher bands, determined by the corresponding Chern number, where the sum of all Chern numbers has to vanish. While this is still true in the effective single-particle model, it does not cover the full physics in the composite-particle setting. Here, excited composite-particle solutions might be unstable (compare Fig. 6); i.e., the soliton can be energetically degenerate with extended, i.e., not self-bound many-particle, states. In such a case, the state would not survive in the real time evolution of the pump, because the soliton can evaporate and, therefore, lose its composite structure.

If, on the other hand, an excited soliton is stable, there is quantized topological transport determined by the effective Chern number of the excited soliton band; see, e.g., Fig. 1(a) in the extended data of Ref. [6]. In Fig. 8, we show the energy spectrum from the three-site soliton ansatz of the AAH model for $N = 3$ particles with a $p = 17$ unit cell and a $k = 8$ phase offset. The interaction strength is chosen as $U/J = 1/3$. As one can see, there are crossing solutions in the low-lying part of the spectrum, above which another gapped soliton solution exists (marked in red). The corresponding Chern number of this soliton band is $C = 2$, which is in agreement with the displayed transport.

VIII. SUMMARY AND OUTLOOK

We developed a full quantum description of topological pumps of self-bound N-particle states, i.e., lattice solitons. The quantum description allowed us to identify and to explicitly calculate a topological invariant, i.e., an effective

single-particle Chern number or Wilson loop explaining the emergence of integer and fractional transport in the full range of interaction strength, where perturbative arguments [14,16] fail. Transitions between phases of differently quantized topological transport observed in experiments [6,13] as well as the possibility of parameter regimes without quantized transport were explained by coalescence of soliton bands and possible degeneracies with extended states. Quantized topological transport can also be observed in excited soliton bands, provided these bands are gapped and stable; i.e., there are no degeneracies with extended many-particle states. The concept can easily be extended to multicomponent solitons [22,23,43], where, among other things, fractional transport was predicted despite the fact that all single-particle bands are topologically trivial. In the latter case, interactions lead not only to the modification of topological properties, such as the transition from integer to fractional phases, but to the *emergence* of topology. Finally, we note that the concept can also be applied to bound many-particle states in cold gas experiments and topological pumps [39,44–47].

Some of the data in this script have been obtained using the QuantumOptics.jl framework [48].

ACKNOWLEDGMENTS

The authors thank Alaa Bayazeed for fruitful discussions. Financial support from the DFG through SFB TR 185, Project No. 277625399, is gratefully acknowledged. The authors also thank the Allianz für Hochleistungsrechnen (AHRP) for giving us access to the "Elwetritsch" HPC Cluster.

DATA AVAILABILITY

The data that support the findings of this article are not publicly available upon publication because it is not technically feasible and/or the cost of preparing, depositing, and hosting the data would be prohibitive within the terms of this research project. The data are available from the authors upon reasonable request.

APPENDIX: EFFECTIVE SOLITON HAMILTONIANS IN THE LIMIT OF STRONGLY LOCALIZED SOLITONS

To derive an effective model for strongly localized composite particles, let us first look at the binding energy of such a maximally localized soliton in the AAH model (1) (i.e., a localization length ξ smaller than the lattice spacing), which has a binding energy given by

$$E_{\mathrm{int},N} = \frac{U}{2} N(N-1), \tag{A1}$$

whereas states with $N-1$ localized particles have an energy

$$E_{\mathrm{int},N-1} = \frac{U}{2}(N-1)(N-2). \tag{A2}$$

The energy difference $|E_{\mathrm{int},N} - E_{\mathrm{int},N-1}|$ is $U(N-1)$. So if U is sufficiently larger than the Bose-enhanced hopping $\sqrt{N}J$, the energetically lowest states are localized solitons.

To derive an effective description of the maximally localized solitons, as proposed in Eq. (18), we have to identify the relevant processes, treating the particle hopping as perturbation. These processes have to be resonant between the degenerate ground states of the interaction Hamiltonian $\mathcal{H}_{\mathrm{int}}$ [35]: For the effective potential, it is the virtual hopping of a single-particle occurring in second-order perturbation theory:

$$\sim \hat{a}_l^\dagger \hat{a}_{l+1} \hat{a}_{l+1}^\dagger \hat{a}_l |\Psi\rangle.$$

On the other hand, the effective hopping of the complete composite particle emerges only in Nth-order perturbation theory:

$$\sim (\hat{a}_{l+1}^\dagger \hat{a}_l)^N |\Psi\rangle.$$

The amplitude for the virtual hopping scales as $\sim 1/U$, while the effective hopping goes with $\sim 1/U^{N-1}$.

The minimal particle number: Triplons—In the following, we explicitly calculate an effective Hamiltonian for the minimal possible particle number: the triplon. For a composite object consisting of only two particles, both processes (virtual and effective hopping) would have the same scaling $1/U$ and, therefore, the interaction has no qualitative influence on the system properties.

The effective potential is calculated directly within second-order perturbation theory of the Hamiltonian and is given as

$$\epsilon_{l,\mathrm{eff}} = \frac{3}{2} \frac{J_{l-1}^2 + J_l^2}{U}. \tag{A3}$$

Calculating the effective triplon hopping in perturbation theory is possible but already requires good bookkeeping since it is a third-order process.

Therefore, we take a look at the local basis of two sites for three particles:

$$|30\rangle, |21\rangle, |12\rangle, |03\rangle.$$

The local Hamiltonian for these states can be written in matrix form:

$$\begin{pmatrix} -3U & -\sqrt{3}J_l & 0 & 0 \\ -\sqrt{3}J_l & -U & -2J_l & 0 \\ 0 & -2J_l & -U & -\sqrt{3}J_l \\ 0 & 0 & -\sqrt{3}J_l & -3U \end{pmatrix}.$$

Here, we assume—without loss of generality—that the left site is located at position l in our system. Diagonalizing this 4×4 matrix yields four eigenstates. The two low-energy eigenstates are (for sufficient large values of the interaction strength U)

$$|\psi_\pm\rangle \propto |30\rangle \pm |03\rangle.$$

The corresponding eigenenergies are

$$E_\pm \propto \mp\, t - 2U - \sqrt{4t^2 \mp 2tU + U^2}.$$

In the effective Hamiltonian [compare Eq. (18)], the eigenenergies of $|\psi_\pm\rangle$ can be shown to be

$$\begin{aligned} E_{\mathrm{eff},\pm} &= \mp J_{l,\mathrm{eff}} + \mathrm{const}, \\ E_{\mathrm{eff},+} - E_{\mathrm{eff},-} &= -2J_{l,\mathrm{eff}}. \end{aligned}$$

Given these two relations, we can Taylor expand the energy difference $E_+ - E_-$ for small values of the hopping amplitude and extract the effective hopping:

$$J_{l,\mathrm{eff}} = -\frac{E_+ - E_-}{2} = \frac{3}{2}\frac{J_l^3}{U^2} + \mathcal{O}\left(\frac{J_l^5}{U^4}\right). \tag{A4}$$

With both the virtual and the effective hopping Eqs. (A3) and (A4), we can calculate an effective single-particle Hamiltonian [Eq. (18)] reflecting the same physics as the full model in the strong interacting limit.

[1] K. v. Klitzing, G. Dorda, and M. Pepper, *New method for high-accuracy determination of the fine-structure constant based on quantized Hall resistance*, Phys. Rev. Lett. **45**, 494 (1980).

[2] D. J. Thouless, *Quantization of particle transport*, Phys. Rev. B **27**, 6083 (1983).

[3] R. Citro and M. Aidelsburger, *Thouless pumping and topology*, Nat. Rev. Phys. **5**, 87 (2023).

[4] Y. Lumer, Y. Plotnik, M. C. Rechtsman, and M. Segev, *Self-localized states in photonic topological insulators*, Phys. Rev. Lett. **111**, 243905 (2013).

[5] S. Mukherjee and M. C. Rechtsman, *Observation of Floquet solitons in a topological bandgap*, Science **368**, 856 (2020).

[6] M. Jürgensen, S. Mukherjee, and M. C. Rechtsman, *Quantized nonlinear Thouless pumping*, Nature (London) **596**, 63 (2021).

[7] V. E. Korepin, N. Bogoliubov, and A. Izergin, *Quantum Inverse Scattering Method and Correlation Functions* (Cambridge University Press, Cambridge, England, 1997), Vol. 3.

[8] D. C. Mattis, *The few-body problem on a lattice*, Rev. Mod. Phys. **58**, 361 (1986).

[9] L. Barbiero and L. Salasnich, *Quantum bright solitons in a quasi-one-dimensional optical lattice*, Phys. Rev. A **89**, 063605 (2014).

[10] S. Aubry and G. André, *Analyticity breaking and anderson localization in incommensurate lattices*, Ann. Isr. Phys. Soc. **3**, 18 (1980).

[11] P. G. Harper, *Single band motion of conduction electrons in a uniform magnetic field*, Proc. Phys. Soc. London Sect. A **68**, 874 (1955).

[12] Y. E. Kraus, Y. Lahini, Z. Ringel, M. Verbin, and O. Zilberberg, *Topological states and adiabatic pumping in quasicrystals*, Phys. Rev. Lett. **109**, 106402 (2012).

[13] M. Jürgensen, S. Mukherjee, C. Jörg, and M. C. Rechtsman, *Quantized fractional Thouless pumping of solitons*, Nat. Phys. **19**, 420 (2023).

[14] M. Jürgensen and M. C. Rechtsman, *Chern number governs soliton motion in nonlinear Thouless pumps*, Phys. Rev. Lett. **128**, 113901 (2022).

[15] D. Zhou, D. Z. Rocklin, M. Leamy, and Y. Yao, *Topological invariant and anomalous edge modes of strongly nonlinear systems*, Nat. Commun. **13**, 3379 (2022).

[16] N. Mostaan, F. Grusdt, and N. Goldman, *Quantized topological pumping of solitons in nonlinear photonics and ultracold atomic mixtures*, Nat. Commun. **13**, 5997 (2022).

[17] T. Tuloup, R. W. Bomantara, and J. Gong, *Breakdown of quantization in nonlinear Thouless pumping*, New J. Phys. **25**, 083048 (2023).

[18] X. Hu, Z. Li, A.-X. Chen, and X. Luo, *Pumping of matter wave solitons in one-dimensional optical superlattices*, New J. Phys. **26**, 123006 (2024).

[19] K. Sone, M. Ezawa, Y. Ashida, N. Yoshioka, and T. Sagawa, *Nonlinearity-induced topological phase transition characterized by the nonlinear Chern number*, Nat. Phys. **20**, 1164 (2024).

[20] K. Sone, M. Ezawa, Z. Gong, T. Sawada, N. Yoshioka, and T. Sagawa, *Transition from the topological to the chaotic in the nonlinear Su–Schrieffer–Heeger model*, Nat. Commun. **16**, 422 (2025).

[21] F. Lederer, G. I. Stegeman, D. N. Christodoulides, G. Assanto, M. Segev, and Y. Silberberg, *Discrete solitons in optics*, Phys. Rep. **463**, 1 (2008).

[22] Y.-L. Tao, J.-H. Wang, and Y. Xu, *Anomalous quantized nonlinear Thouless pumping*, arXiv:2409.19515.

[23] Y.-L. Tao, Y. Zhang, and Y. Xu, *Nonlinearity-induced fractional Thouless pumping of solitons*, Phys. Rev. Lett. **135**, 097202 (2025).

[24] M. Jürgensen, J. Steiner, G. Refael, and M. C. Rechtsman, *Multi-band fractional Thouless pumps*, arXiv:2504.09338 [Phys. Rev. Lett. (to be published)].

[25] Q. Fu, P. Wang, Y. V. Kartashov, V. V. Konotop, and F. Ye, *Nonlinear Thouless pumping: Solitons and transport breakdown*, Phys. Rev. Lett. **128**, 154101 (2022).

[26] A. Altland and M. R. Zirnbauer, *Nonstandard symmetry classes in mesoscopic normal-superconducting hybrid structures*, Phys. Rev. B **55**, 1142 (1997).

[27] S. Ryu, A. P. Schnyder, A. Furusaki, and A. W. Ludwig, *Topological insulators and superconductors: Tenfold way and dimensional hierarchy*, New J. Phys. **12**, 065010 (2010).
[28] P. Naldesi, J. P. Gomez, B. Malomed, M. Olshanii, A. Minguzzi, and L. Amico, *Rise and fall of a bright soliton in an optical lattice*, Phys. Rev. Lett. **122**, 053001 (2019).
[29] M. C. Gutzwiller, *Effect of correlation on the ferromagnetism of transition metals*, Phys. Rev. Lett. **10**, 159 (1963).
[30] D. J. Thouless, M. Kohmoto, M. P. Nightingale, and M. den Nijs, *Quantized Hall conductance in a two-dimensional periodic potential*, Phys. Rev. Lett. **49**, 405 (1982).
[31] Q. Niu, D. J. Thouless, and Y.-S. Wu, *Quantized Hall conductance as a topological invariant*, Phys. Rev. B **31**, 3372 (1985).
[32] F. Wilczek and A. Zee, *Appearance of gauge structure in simple dynamical systems*, Phys. Rev. Lett. **52**, 2111 (1984).
[33] A. Scott, J. Eilbeck, and H. Gilhøj, *Quantum lattice solitons*, Physica (Amsterdam) **78D**, 194 (1994).
[34] Y. Ke, X. Qin, Y. S. Kivshar, and C. Lee, *Multiparticle Wannier states and Thouless pumping of interacting bosons*, Phys. Rev. A **95**, 063630 (2017).
[35] F. Mila and K. P. Schmidt, *Strong-coupling expansion and effective Hamiltonians*, in *Introduction to Frustrated Magnetism* (Springer, Berlin Heidelberg, 2010), pp. 537–559.
[36] M. J. Rice and E. J. Mele, *Elementary excitations of a linearly conjugated diatomic polymer*, Phys. Rev. Lett. **49**, 1455 (1982).
[37] M. Lohse, C. Schweizer, O. Zilberberg, M. Aidelsburger, and I. Bloch, *A Thouless quantum pump with ultracold bosonic atoms in an optical superlattice*, Nat. Phys. **12**, 350 (2016).
[38] A. Hayward, C. Schweizer, M. Lohse, M. Aidelsburger, and F. Heidrich-Meisner, *Topological charge pumping in the interacting bosonic Rice-Mele model*, Phys. Rev. B **98**, 245148 (2018).
[39] M. Valiente and D. Petrosyan, *Two-particle states in the Hubbard model*, J. Phys. B **41**, 161002 (2008).
[40] J. Tangpanitanon, V. M. Bastidas, S. Al-Assam, P. Roushan, D. Jaksch, and D. G. Angelakis, *Topological pumping of photons in nonlinear resonator arrays*, Phys. Rev. Lett. **117**, 213603 (2016).
[41] B. Huang, Y. Ke, W. Liu, and C. Lee, *Topological pumping induced by spatiotemporal modulation of interaction*, Phys. Scr. **99**, 065997 (2024).
[42] S. Hu, Y. Ke, Y. Deng, and C. Lee, *Dispersion-suppressed topological Thouless pumping*, Phys. Rev. B **100**, 064302 (2019).
[43] H. Lyu, Y. Zhang, and T. Busch, *Thouless pumping and trapping of two-component gap solitons*, Phys. Rev. Res. **6**, L042010 (2024).
[44] K. Winkler, G. Thalhammer, F. Lang, R. Grimm, J. Hecker Denschlag, A. Daley, A. Kantian, H. Büchler, and P. Zoller, *Repulsively bound atom pairs in an optical lattice*, Nature (London) **441**, 853 (2006).
[45] E. Bertok, F. Heidrich-Meisner, and A. A. Aligia, *Splitting of topological charge pumping in an interacting two-component fermionic Rice-Mele Hubbard model*, Phys. Rev. B **106**, 045141 (2022).
[46] A.-S. Walter, Z. Zhu, M. Gächter, J. Minguzzi, S. Roschinski, K. Sandholzer, K. Viebahn, and T. Esslinger, *Quantization and its breakdown in a Hubbard–Thouless pump*, Nat. Phys. **19**, 1471 (2023).
[47] K. Viebahn, A.-S. Walter, E. Bertok, Z. Zhu, M. Gächter, A. A. Aligia, F. Heidrich-Meisner, and T. Esslinger, *Interactions enable Thouless pumping in a nonsliding lattice*, Phys. Rev. X **14**, 021049 (2024).
[48] S. Krämer, D. Plankensteiner, L. Ostermann, and H. Ritsch, *Quantumoptics.jl: A Julia framework for simulating open quantum systems*, Comput. Phys. Commun. **227**, 109 (2018).